

# Design and Analysis of Decentralized Dynamic Sliding Mode Controller for TITO Process

M. G. Ghogare <sup>a,1,\*</sup>, A. R. Laware <sup>b,2</sup>, S. L. Patil <sup>c,3</sup>, C. Y. Patil <sup>d,4</sup>

<sup>a,c,d</sup> College of Engineering Pune, India

<sup>b</sup> Dr. Vikhe Patil College of Engineering, Ahmednagar, India

<sup>1</sup> [mukeshghogare@gmail.com](mailto:mukeshghogare@gmail.com); <sup>2</sup> [ajitlaware2003@gmail.com](mailto:ajitlaware2003@gmail.com); <sup>3</sup> [slp.instru@coep.ac.in](mailto:slp.instru@coep.ac.in);

<sup>4</sup> [cyp.instru@coep.ac.in](mailto:cyp.instru@coep.ac.in)

\* Corresponding Author

## ARTICLE INFO

### Article History

Received March 28, 2022

Revised April 25, 2022

Accepted April 28, 2022

### Keywords

Decentralized controller;

Dynamic sliding mode controller;

Two-input two-output system;

Real-time experimentation

## ABSTRACT

In this paper, a decentralized dynamic sliding mode control (DySMC) strategy is applied to a multivariable level control system. The time derivative of the control input of the DySMC is considered a new control variable for an augmented system which is composed of the original system and the integrator. This DySMC can transfer discontinuous terms to the first-order derivative of the control input and effectively reduce the chattering. The interactions between input/output variables are a common phenomenon and a challenging task in the design of multi-loop controllers for interacting multivariable processes. For reducing the interaction among variables, ideal decouplers are used. Independent diagonal controllers are designed for each decoupled subsystem, which is reduced to the first-order plus dead-time (FOPDT) model. A numerical simulation test has been carried out on a reactor system of the Industrial-Scale Polymerization (ISP). Experimental tests are performed to check the efficacy of the proposed controller using a laboratory-level coupled tank system. A comparison of the proposed approach and sliding mode controller (SMC) is presented. Simulation and experiment results show that the DySMC approach reduces the chattering, and compensates for the effect of the external disturbances, and parametric uncertainties.

This is an open access article under the [CC-BY-SA](https://creativecommons.org/licenses/by-sa/4.0/) license.



## 1. Introduction

Usually, processes in industries are having nonlinear dynamics and they are modeled as a linear two-input two-output (TITO) system. Designing a controller for these systems is somewhat challenging task since they involve time-delay, non-linearity, and interaction among the system variables. In presence of these above parameters, the system will not perform well [1]. Multi-loop controllers are difficult to design and tune in comparison with single-loop controllers, due to the presence of process and loop interactions. The TITO systems are having two types of composition, mainly centralized or full structure and diagonal structure or decentralized structure [2], [3]. OFF-diagonal controllers are designed to remove the interactions among variables in centralized multivariable controllers. But while designing the controller, control elements are increased because of which the tuning of controller becomes a difficult task. For designing centralized controllers different methods have been proposed [4], [5]. In these approaches, interactions among variables are reduced but the loop controllers still interact using full structure controller. Tuning in the centralized controller for individual

loops cannot be done separately because the design process is hampered or it becomes complicated. On the other hand, the decentralized controller method is simple and the design procedure involves only diagonal controllers that need to be tuned. Therefore the single-input single-output (SISO) controllers in multiple single loops is formed which are controlling multi-input multi-output (MIMO) systems [3].

A multivariable systems consists of  $n$  input and  $n$  output variables. It is also called as mono-variable system. In designing the multivariable system, it has two parts. Firstly to minimize the interaction among variables, decouplers are designed. This can be done by finding the diagonal elements. Controllers can be designed using decentralized method. The product of controller matrices and decouplers will be the final control system. The multivariable controller consists of decouplers and single-loop controllers. The importance of decouplers is that they eliminates the interaction.

Due to the easiest way and simple designing, PID controllers with decouplers are very much popular in process industries. For TITO processes, decentralized PID controllers are widely used with time delay. Various decouplers are reported in [6], [7]. Most of these PID controllers uses the first-order plus dead-time (FOPDT) or second-order plus dead-time (SOPDT) model, which has reduced linear structure. Using FOPDT and SOPDT models of PID controller, there is an introduction of unreliable parameters which produces larger overshoots and settling time. Against parametric uncertainty and external disturbances, the controller is not robust.

SMC a discontinuous control has many advantages such as, parametric variations, can handle the uncertainties and unknown disturbances. Chattering is the main disadvantage of SMC, as control switching occurs at high frequency with infinite duration. For practical cases, this switching is not possible due to presence of time delay in the system. It may cause damage to the actuators and final control elements [8]. System stability may not be achieved. The presence of the chattering effect generates inappropriate control laws for actuators for process application. 'sign' function used in designing of SMC controller, is a discontinuous component which causes the chattering [9], [10].

To remove the chattering effect two methods are reported. In first method, discontinuous control is replaced by continuous one by adding a boundary layer near the sliding variable [11], [12] using saturation function, hyperbolic function or sigmoid function [8]. Second method uses auxiliary control input into the system for eliminating chattering effect [12], [13]. Both the methods eliminates the chattering, but a finite steady state error condition may exist, due to which perfect disturbance rejection cannot be guaranteed.

To eliminate the effect of chattering using DySMC [14], [15], [16], [17], an integrator is used in front of the system. The new control variable in DySMC is a time derivative of the control input. So the overall system includes, original system and integrator. This increases the size of system. Using an integrator in DySMC controller, there is a reduction in chattering and also no boundary layer condition is used while designing. Therefore, the perfect disturbance rejection is guaranteed. DySMC overcomes the limitation of traditional SMC and provides improved accuracy. Also, it provides an improved system stability, obtaining better system performances even under external disturbances or parametric uncertainties.

This paper aims in designing a decentralized DySMC controller for the TITO system. Decoupled subsystems are formed in which ideal decouplers are used for reducing the interactions among the variables. For obtaining the desired controller, each subsystem has been reduced to FOPDT model. Frequency fitting method at two different frequencies is used for obtaining the FOPDT model of the system [18]. Each decoupled subsystem has independently designed SISO DySMC. The proposed controller solves the main SMC problem of chattering and presents a simple and easy synthesis method for the controller design and simplifying its implementation. To explore the effectiveness of the proposed controller, a numerical simulation test is carried on a reactor system of ISP. The proposed controllers performance is validated by conducting an experiment on a laboratory level control

system. Very limited literature is available which gives the usage of DySMC for process application mainly for TITO systems. The performance of the proposed design is found to be better and robust for disturbances and uncertainties. The research contribution is to design a decentralized DySMC controller for a multivariable system having interactions among the variables. To eliminate the interactions decouplers have been designed firstly and then implemented on TITO system.

The paper is organized as follows: Section 2 gives the design procedure of decoupling. In Section 3, decentralized controller for multivariable process is discussed in brief. In Section 4, dynamic sliding mode control design is explained with stability analysis. Simulation studies are given in Section 5 to prove the performance. Section 6 presents the real-time experimentation with experimental results to validate the performance of the controller. Conclusions are provided in Section 7.

### 2. Decoupler Design

Decouplers are used to remove the interactions among the variables in multivariable systems. Using decouplers independent control loops can be designed. There are different decoupling methods, but linear decoupling is mostly used.

The basic block diagram of TITO system is shown in Fig. 1. The closed-loop system matrix is,

$$\begin{bmatrix} y_1 \\ y_2 \end{bmatrix} = \begin{bmatrix} G_{11} & G_{12} \\ G_{21} & G_{22} \end{bmatrix} \begin{bmatrix} G_{C1} & 0 \\ 0 & G_{C2} \end{bmatrix} \begin{bmatrix} r_1 - y_1 \\ r_2 - y_2 \end{bmatrix} \tag{1}$$

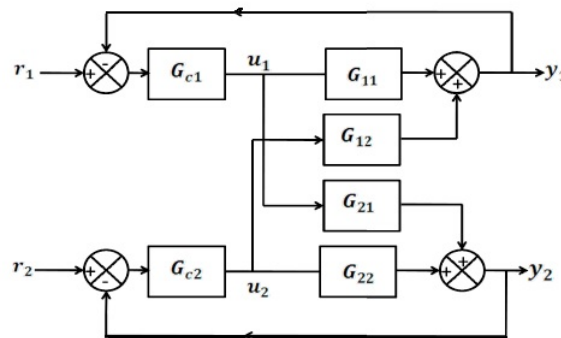


Fig. 1. Basic block diagram of 2X2 system

In Eq. (1),  $G_{12}$  and  $G_{21}$  are inter-connected with each other. To remove the interaction among them using decoupler, the controller output is transformed to matrix  $D(s)$ , which contains the decoupling functions. This is done using manipulated variables given as

$$\begin{bmatrix} u_1 \\ u_2 \end{bmatrix} = \begin{bmatrix} d_{11} & d_{12} \\ d_{21} & d_{22} \end{bmatrix} \begin{bmatrix} G_{C1} & 0 \\ 0 & G_{C2} \end{bmatrix} \begin{bmatrix} r_1 - y_1 \\ r_2 - y_2 \end{bmatrix} \tag{2}$$

and the system Eq. (1) can be written as

$$\begin{bmatrix} y_1 \\ y_2 \end{bmatrix} = \begin{bmatrix} G_{11} & G_{12} \\ G_{21} & G_{22} \end{bmatrix} \begin{bmatrix} d_{11} & d_{12} \\ d_{21} & d_{22} \end{bmatrix} \begin{bmatrix} G_{C1} & 0 \\ 0 & G_{C2} \end{bmatrix} \begin{bmatrix} r_1 - y_1 \\ r_2 - y_2 \end{bmatrix} \tag{3}$$

$$= G(s)D(s)G_C(s) \begin{bmatrix} r_1 - y_1 \\ r_2 - y_2 \end{bmatrix} \tag{4}$$

where  $G(s)D(s)G_C(s)$  should be a diagonal matrix. Therefore,  $G_0(s) = G(s)D(s)G_C(s)$ . On solving Eq. (3) and Eq. (4) for  $y$ :

$$\begin{bmatrix} y_1 \\ y_2 \end{bmatrix} = [1 + G_0]^{-1}G_0 \begin{bmatrix} r_1 \\ r_2 \end{bmatrix} \tag{5}$$

Since  $G_0$  is diagonal, the matrix  $[1 + G_0]^{-1}G_0$  is also diagonal. Then,

$$\begin{bmatrix} G_{11} & G_{12} \\ G_{21} & G_{22} \end{bmatrix} \begin{bmatrix} d_{11} & d_{12} \\ d_{21} & d_{22} \end{bmatrix} = \begin{bmatrix} H_1 & 0 \\ 0 & H_2 \end{bmatrix} \quad (6)$$

From Eq. (6), the elements of  $D(s)$  can be found as

$$d_{11} = \frac{G_{22}H_1}{G_{11}G_{22} - G_{12}G_{21}} \quad (7)$$

$$d_{22} = \frac{G_{11}H_2}{G_{11}G_{22} - G_{12}G_{21}} \quad (8)$$

$$d_{12} = \frac{-G_{12}}{G_{11}}d_{22} \quad (9)$$

$$d_{21} = \frac{-G_{21}}{G_{22}}d_{11} \quad (10)$$

By assuming

$$H_1 = \frac{G_{11}G_{22} - G_{12}G_{21}}{G_{22}} \quad (11)$$

$$H_2 = \frac{G_{11}G_{22} - G_{12}G_{21}}{G_{11}} \quad (11)$$

To eliminate the interactions among all loops, elements of a TITO system for decoupling matrix are determined by,

$$d_{11} = 1 \quad (12)$$

$$d_{12} = -\frac{g_{12}}{g_{11}} \quad (13)$$

$$d_{21} = -\frac{g_{21}}{g_{22}} \quad (14)$$

$$d_{22} = 1 \quad (15)$$

Combining the diagonal controller  $K_d(s)$  with a block compensator  $D(s)$ , a decentralized control system is designed, in which controller manipulates the variable  $u_i^*$  instead of  $u_i$  as shown in Fig. 2. with this configuration the controller see the process as a set of  $n$  completely independent process or with minimum interaction.

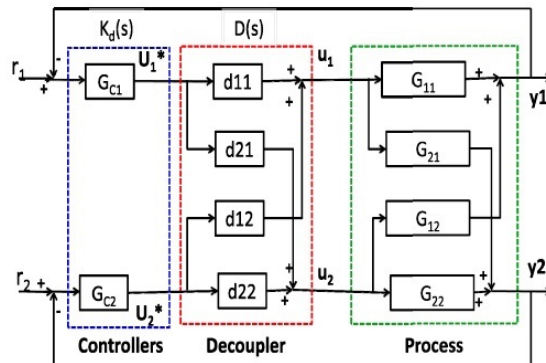


Fig. 2. System with decoupler and single-loop controllers

### 3. Decentralized Controller for Multivariable Process

Fig. 3 illustrates the generalized composition of TITO process with decoupler. Consider open-loop transfer function of TITO system as

$$G_p(s) = \begin{bmatrix} G_{p11}(s) & G_{p12}(s) & \dots & G_{p1n}(s) \\ G_{p21}(s) & G_{p22}(s) & \dots & G_{p2n}(s) \\ \vdots & \vdots & \vdots & \vdots \\ G_{pn1}(s) & G_{pn2}(s) & \dots & G_{pnn}(s) \end{bmatrix} \quad (16)$$

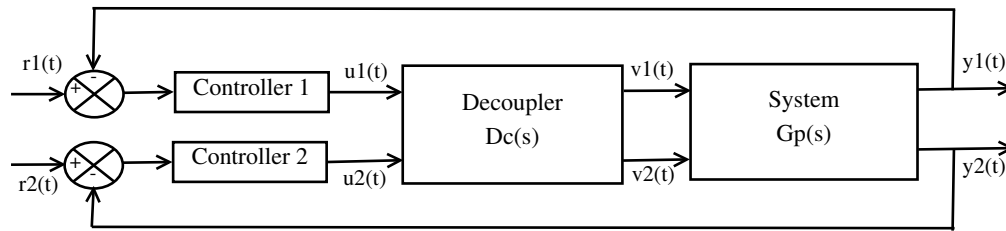


Fig. 3. Block diagram of decentralized controller

An ideal decoupler is,

$$D_c(s) = \begin{bmatrix} D_{c11}(s) & D_{c12}(s) & \dots & D_{c1n}(s) \\ D_{c21}(s) & D_{c22}(s) & \dots & D_{c2n}(s) \\ \vdots & \vdots & \vdots & \vdots \\ D_{cn1}(s) & D_{cn2}(s) & \dots & D_{cnn}(s) \end{bmatrix} \quad (17)$$

The equivalent multiloop SISO structure is,

$$F(s) = G_p(s)D_c(s) \quad (18)$$

where,  $F(s)$  is a diagonal matrix represented by,

$$F(s) = \begin{bmatrix} F_{11}(s) & 0 & \dots & 0 \\ 0 & F_{22}(s) & \dots & 0 \\ \vdots & \vdots & \vdots & \vdots \\ 0 & 0 & \dots & F_{nn}(s) \end{bmatrix} \quad (19)$$

Decoupler in Eq. (17) can be represented as [6]

$$D_e(s) = Adj[G_p(s)]Q(s) \quad (20)$$

where  $F(s)$  is a diagonal matrix.  $D_c(s)$  and  $Q(s)(q_i(s))$  elements are obtained by removing the pole-zero, dead-time, and gain of  $i^{th}$  column of  $Adj[G_p(s)]$ , which are common in that [3]. Their inverse can be incorporated in  $q_i(s)$ . From Eq. (21), the dead time in  $F(s)$  is calculated by using Taylor series approximation and is given by,

$$e^{-T_d s} \cong \frac{1}{T_d s + 1} \quad (21)$$

where  $T_d$  is the dead-time of the process. By Taylor's approximation, all the delays are converted into pole form and the decoupled system in Eq. (18) can be given as

$$F_i(s) = \frac{b_{0i}s^{m_i} + b_{1i}s^{(m-1)_i} + \dots + b_{m_i}}{s^{n_i} + a_{1i}s^{(n-1)_i} + \dots + a_{n_i}} \quad (22)$$

where  $m \leq n$ ,  $a_i$ 's and  $b_i$ 's are the coefficients of polynomial.

### 3.1. Model Order Reduction

Eq. (22) gives the higher-order controller design for the decoupled system. For designing DySMC, this equation should be reduced to the FOPDT model. FOPDT model for higher processes involves the parameters such as process gain, dead-time, and time constant [19]. For each decoupled subsystem, the FOPDT model is given by,

$$G_i(s) = \frac{q_i e^{-\tau_i s}}{T_i s + 1}, \quad i = 1, 2. \quad (23)$$

To find the FOPDT model for  $F_i(s)$ , three parameters,  $q_i$  (gain of process),  $T_i$  (time constant) and  $\tau_i$  (dead time) in Eq. (23), are unknown and have to be found out. Using frequency response fitting method at two points,  $\omega = 0$  and  $\omega = \omega_{ci}$ , where,  $\omega_{ci}$  is the phase crossover frequency [18], the FOPDT model parameters can be determined. On solving for two frequencies,

$$\begin{aligned} G_i(0) &= F_i(0) \\ |G_i(j\omega_{ci})| &= |F_i(j\omega_{ci})| \\ \angle G_i(j\omega_{ci}) &= \angle F_i(j\omega_{ci}) \end{aligned} \quad (24)$$

FOPDT model parameters are given by [7],

$$\begin{aligned} Q_i &= F_i(0) \\ T_i &= \sqrt{\frac{Q_i^2 - |F_i(j\omega_{ci})|^2}{|F_i(j\omega_{ci})|^2 \omega_{ci}^2}} \\ \tau_i &= \frac{\pi + \tan^{-1}(-\omega_{ci} T_i)}{\omega_{ci} T_i} \end{aligned} \quad (25)$$

### 4. Dynamic Sliding Mode Controller (DySMC)

In order to eliminate the chattering effect by the dynamic sliding mode approach, the switching function of the normal sliding mode is transformed to new switching function. This new function may be relatively first-order or higher-order derivative. The discontinuous terms are shifted to first or higher-order derivative in the control input [20], [21], [22]. DySMC synthesis has received attention in recent years whereby introducing extra dynamics into a sliding surface which helps to solve the difficulties in practice. DySMC controller as the conventional sliding mode control (SMC) has two components: a continuous part (sliding mode) and a discontinuous part (or reaching mode) [20], [21], [23], [24].

$$\dot{u}_{DySMC}(t) = \dot{u}_c(t) + \dot{u}_d(t) \quad (26)$$

Integrating the discontinuous part of the controller, the DySMC attenuates the effect of the chattering and improves the system's reaching phase time as

$$\dot{u}_d(t) = k_D \text{sgn}(s(t)) \quad (27)$$

Consider a process model of uncertain system given as [21], [25],

$$\begin{aligned} \dot{x}_1(t) &= x_2(t) \\ \dot{x}_2(t) &= p(x, t) + q(x, t)u(t) + \Delta p(x, t) + \\ &\quad \Delta q(x, t)u(t) + \delta(x, t) \\ y(t) &= x_1(t) \end{aligned} \quad (28)$$

where  $x_1(t)$  and  $x_2(t)$  are the state variables.  $x(t)$  is the state vector,  $y(t)$  is the system output,  $u(t)$  is the control input,  $p(x, t)$ ,  $q(x, t)$  are known system functions,  $\Delta p(x, t)$ ,  $\Delta q(x, t)$  are uncertainties in  $p(x, t)$ ,  $q(x, t)$  and  $\delta(x, t)$  is an external disturbance.

System uncertainties  $\Delta p(x, t)$ ,  $\Delta q(x, t)$  and disturbance  $\delta(x, t)$  satisfies the following matching conditions [26], [27],

$$\Delta p(x, t) + \Delta q(x, t) + \delta(x, t) = q(x, t)d(x, t) \quad (29)$$

where  $d(x, t)$  represents uncertainties in estimated plant parameters.

Eq. (28) can be rewritten as

$$\begin{aligned} \dot{x}_1(t) &= x_2(t) \\ \dot{x}_2(t) &= p(x, t) + q(x, t)u(t) + d(x, t) \\ y(t) &= x_1(t) \end{aligned} \quad (30)$$

In designing of DySMC,  $e(t)$  [28], [29] is tracking error and  $s(t)$  is sliding surface are given by,

$$\begin{aligned} e(t) &= y(t) - y_d(t) \\ s(t) &= ce(t) + \dot{e}(t) \end{aligned} \quad (31)$$

where  $y_d(t)$  and  $c$  are desired output and positive real constant respectively.

$$\dot{s}(t) = p(x, t) + q(x, t)u(t) + d(x, t) - \dot{y}_d + c\dot{e}(t) \quad (32)$$

Construct the new dynamic changing surface as

$$\sigma(t) = \dot{s}(t) + \lambda s(t) \quad (33)$$

where  $\lambda > 0$ , when  $\sigma(t) = 0$ ,  $\dot{s}(t) + \lambda s(t) = 0$  is a asymptotically stable, therefore  $e(t) \rightarrow 0$  and  $\dot{e}(t) \rightarrow 0$ .

Rewriting Eq. (32) and Eq. (33) as

$$\begin{aligned} \sigma(t) &= \dot{s}(t) + \lambda s(t) \\ &= p(x, t) + q(x, t)u + d(x, t) - \dot{y}_d + c\dot{e} + \lambda s(t) \end{aligned}$$

The dynamic controller is selected as

$$\begin{aligned} \dot{u}(t) &= \frac{1}{q(x, t)}(-\dot{p}(x, t) + (c + \lambda)\ddot{y}_d + \ddot{y}_d - \\ &(\dot{q}(x, t) + cq(x, t) + \lambda q(x, t)u) - (c + \lambda)p(x, t) - \\ &\lambda c\dot{e} - \rho \operatorname{sgn}(\sigma)) \end{aligned} \quad (34)$$

where,  $\rho > 0$ .

#### 4.1. Stability Analysis

A Lyapunov function is considered for stability analysis and given as [30]

$$V(t) = \frac{1}{2}\sigma^2(t) \quad (35)$$

Assumptions is  $V(t) > 0$ . The derivative of  $V$  is calculated as

$$\dot{V}(t) = \sigma(t)\dot{\sigma}(t) \quad (36)$$

Eq. (34) yields,

$$\dot{\sigma}(t) = \dot{d}(t) + (c + \lambda)d(x, t) - \rho \operatorname{sgn}(\sigma(t)) \quad (37)$$

Therefore, Eq. (36) and Eq. (37) gives,

$$\sigma(t)\dot{\sigma}(t) = \sigma(t)(\dot{d}(x, t) + (c + \lambda)d(t)) - \rho|\sigma(t)| \quad (38)$$

For achieving the stability condition  $\sigma\dot{\sigma}$  should be negative definite and also it depends on the selection of  $\rho$ ,  $c$  and  $\lambda$  which is given by,

$$(\dot{d}(x, t) + (c + \lambda)d(x, t))\sigma - \rho|\sigma| < 0 \quad (39)$$

where  $\rho$ ,  $c$  and  $\lambda$  are the tuning parameters. Eq. (39) gives the stability condition. For the system to be stable, this condition should be satisfied.

## 5. Simulation Example

Industrial-scale polymerization (ISP) of a reactor, an example is taken for the simulation study. To check the efficacy of the proposed controller it is compared with conventional SMC. The transfer function of ISP is [31],

$$G_p(s) = \begin{bmatrix} \frac{22.89}{(4.572s + 1)}e^{-0.2s} & \frac{-11.64}{(1.807s + 1)}e^{-0.4s} \\ \frac{4.689}{(2.174s + 1)}e^{-0.2s} & \frac{5.8}{(1.801s + 1)}e^{-0.4s} \end{bmatrix}$$

From Eq. (22), decoupler can be given as [32]

$$D_c(s) = \begin{bmatrix} \frac{5.80}{(1.801s + 1)}e^{-0.2s} & \frac{11.64}{(1.807s + 1)}e^{-0.2s} \\ \frac{-4.689}{2.174s + 1} & \frac{22.89}{4.572s + 1} \end{bmatrix}$$

The decoupled subsystems can be computed by,

$$\begin{aligned} F(s) &= G_p(s)D_c(s) \\ F_{11}(s) &= \frac{132.762}{(4.572s + 1)(1.801s + 1)(0.4s + 1)} + \\ &\quad \frac{54.58}{(1.807s + 1)(2.174s + 1)(0.4s + 1)} \\ F_{12}(s) &= F_{21}(s) = 0 \end{aligned} \quad (40)$$

and

$$F_{22}(s) = \frac{132.762}{(4.572s + 1)(1.801s + 1)(0.4s + 1)} + \frac{54.58}{(1.807s + 1)(2.174s + 1)(0.4s + 1)} \quad (41)$$

Here,  $F_{11}(s) = F_{22}(s)$ , therefore subsystems will have same the controller. FOPDT model for the above system in reduced form is,

$$G_{FOPDT} = \frac{187.3}{12.35s + 1}e^{-1.05s} \quad (42)$$

For decentralized control composition, two DySMC are decoupled together with the plant model. The controller has two control inputs  $u_1$  and  $u_2$ . The setpoints are given by  $r_1, r_2$ , and the plant outputs are taken as  $y_1, y_2$ . Two independent DySMC can be obtained using the above configuration with minimum interactions. Therefore the state space models obtained for DySMC are

$$\ddot{y}_1(t) = -0.0771\dot{y}_1(t) - 1.0334y_1(t) + 0.0006423u_1(t) + d_1(x, t) \quad (43)$$

$$\ddot{y}_2(t) = -0.0771\dot{y}_2(t) - 1.0334y_2(t) + 0.0005418u_2(t) + d_2(x, t) \quad (44)$$

where  $d_1(x, t)$  and  $d_2(x, t)$  are uncertain and external disturbance in the process. By using Eq. (34) control inputs  $u_1$  and  $u_2$  are given from Eq. (43) and Eq. (44) as

$$u_1(t) = \frac{1}{q_1(x, t)}(-\dot{p}_1(x, t) + (c_1 + \lambda_1)\ddot{y}_{d1} + \ddot{y}_{d1} - (\dot{q}_1(x, t) + c_1q_1(x, t) + \lambda_1q_1(x, t)u_1) - (c_1 + \lambda_1)p_1(x, t) - \lambda_1c_1\dot{e}_1 - \rho_1\text{sgn}(\sigma_1)) \quad (45)$$

Also,

$$\begin{aligned} e_1(t) &= y_1 - y_{d1} \\ s_1(t) &= c_1e_1 + \dot{e}_1(t) \\ \sigma_1(t) &= \lambda_1s_1(t) + \dot{s}_1(t) \end{aligned}$$

For simulation studies the values of the constants are selected as,  $c_1 = 5$ ,  $\lambda_1=15$ ,  $\rho_1 = 25$ . Disturbance are added as,  $d_1(x, t) = 1$ , for  $800 \leq t \leq 820$  and  $d_2(x, t) = 1$ , for  $1500 \leq t \leq 1520$ .

$$u_2(t) = \frac{1}{q_2(x, t)}(-\dot{p}_2(x, t) + (c_2 + \lambda_2)\ddot{y}_{d2} + \ddot{y}_{d2} - (\dot{q}_2(x, t) + c_2q_2(x, t) + \lambda_2q_2(x, t)u_2) - (c_2 + \lambda_2)p_2(x, t) - \lambda_2c_2\dot{e}_2 - \rho_2\text{sgn}(\sigma_2)) \quad (46)$$

Also,

$$\begin{aligned} e_2(t) &= y_2 - y_{d2} \\ s_2 &= c_2e_2 + \dot{e}_2 \\ \sigma_2 &= \lambda_2s_2 + \dot{s}_2 \end{aligned}$$

For simulation studies the values of the constants are to be:  $c_2 = 5$ ,  $\lambda_2=15$ ,  $\rho_2 = 31$ . Disturbance are added as,  $d_1(x, t) = 1$ , for  $800 \leq t \leq 820$  and  $d_2(x, t) = 1$ , for  $1500 \leq t \leq 1520$ .

### 5.1. Multi-level Setpoint Test

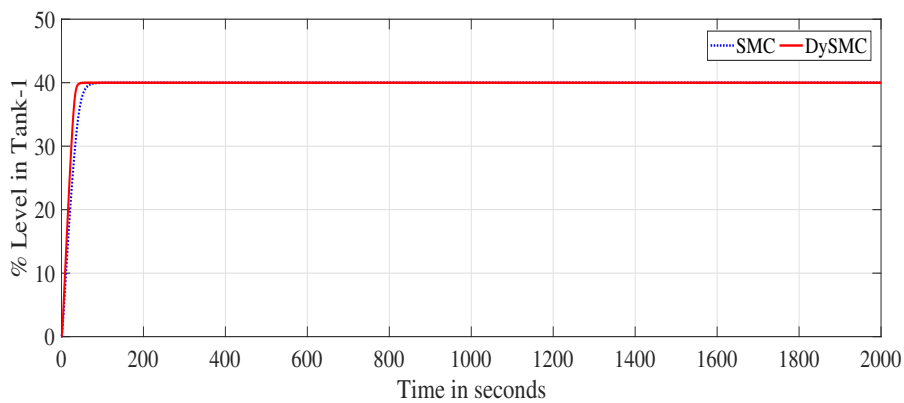
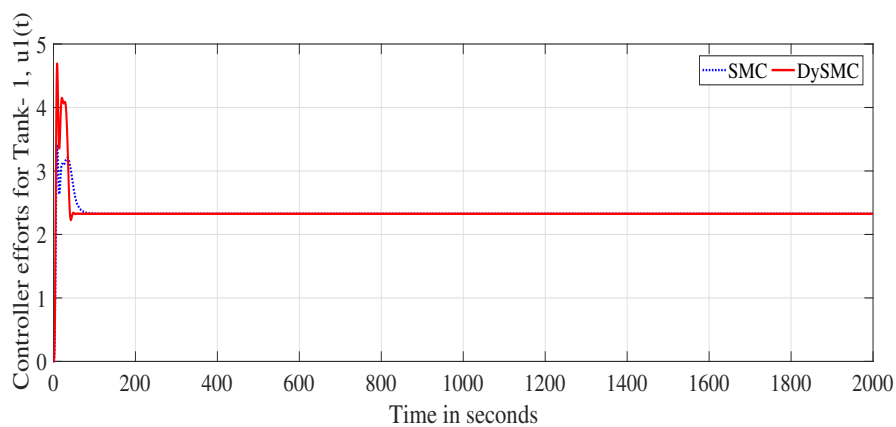
MATLAB/ Simulink platform is used for carrying out the numerical simulation. Fig. 4 and Fig. 5 show the nominal response and the control efforts for Tank-1. Similarly Fig. 6 and Fig. 7 show the responses for Tank-2. Fig. 8 show the output response of Tank-1 when the reference signal is changed from 40% to 50% for 600 seconds to 1000 seconds and 40% to 34% from 1400 seconds to 1700 seconds. Fig. 9 indicates the controller efforts of Tank-1 for setpoint change. Similarly Fig. 10 and Fig. 11 gives the estimated response as well as control efforts for Tank-2 for multi-level setpoint change. Summary of simulation results in tabulated in Table 1 in which time domain specifications such as,  $T_s$  : settling time,  $T_r$  : rise time and  $\%M_p$  : peak overshoot are considered for comparison purpose without parametric uncertainty. Table 2 gives the comparison of performance indices such as,  $IAE$  : Integral absolute error,  $ISE$  : Integral squared error,  $ISTAE$  : Integral squared timed-absolute error and  $ISECE$  : Integral squared error and control error without parametric uncertainty.

**Table 1.** Summary of time domain specifications without parametric uncertainty

Controller	Input ( $u$ ) Output ( $y$ )	Time domain specifications		
		$T_s$	$T_r$	$\%M_p$
DySMC	$u_1 - y_1$	53.97	4.44	0
	$u_2 - y_2$	58.8	4.78	0
SMC	$u_1 - y_1$	88.36	5.48	0
	$u_2 - y_2$	102.71	6.46	0

**Table 2.** Summary of error performance indices without parametric uncertainty

Controller	Input ( $u$ ) Output ( $y$ )	Error indices			
		$IAE$	$ISE$	$ISTAE$	$ISECE$
DySMC	$u_1 - y_1$	26.54	41.28	138.64	93.26
	$u_2 - y_2$	30.12	43.17	181.72	107.83
SMC	$u_1 - y_1$	29.75	43.78	252.34	98.37
	$u_2 - y_2$	34.45	45.67	283.36	102.56

**Fig. 4.** Output response,  $y_1$ **Fig. 5.** Controller efforts,  $u_1$

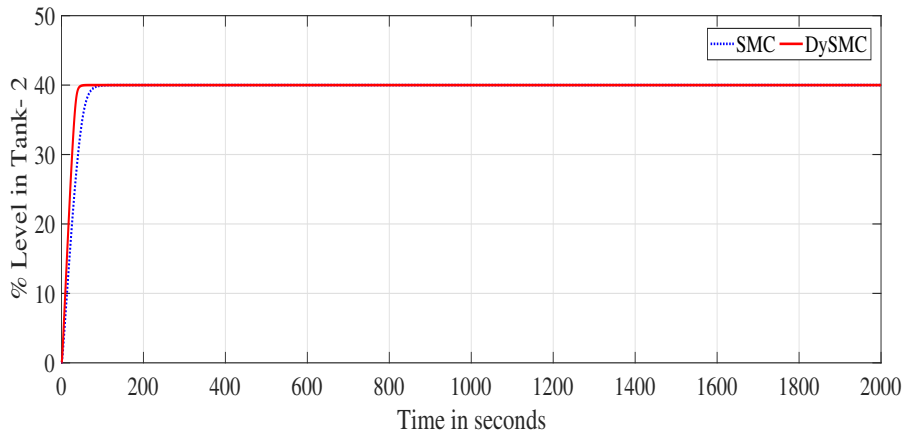


**Fig. 6.** Output response,  $y_2$

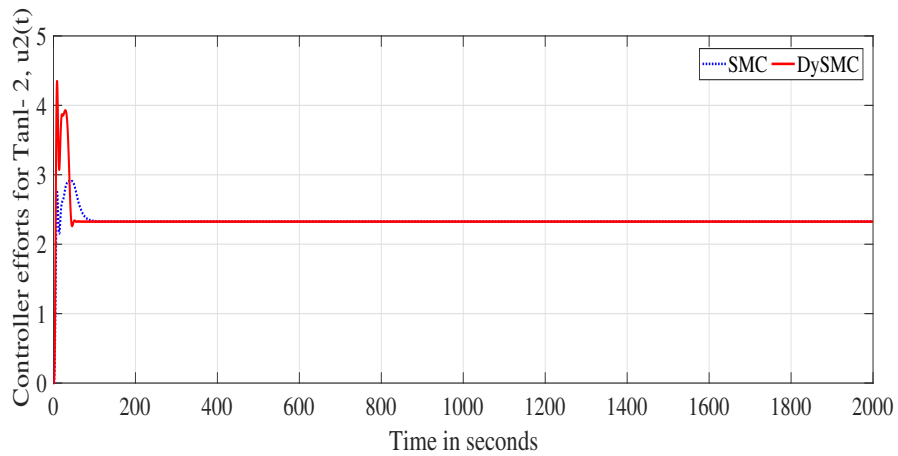


**Fig. 7.** Controller efforts,  $u_2$

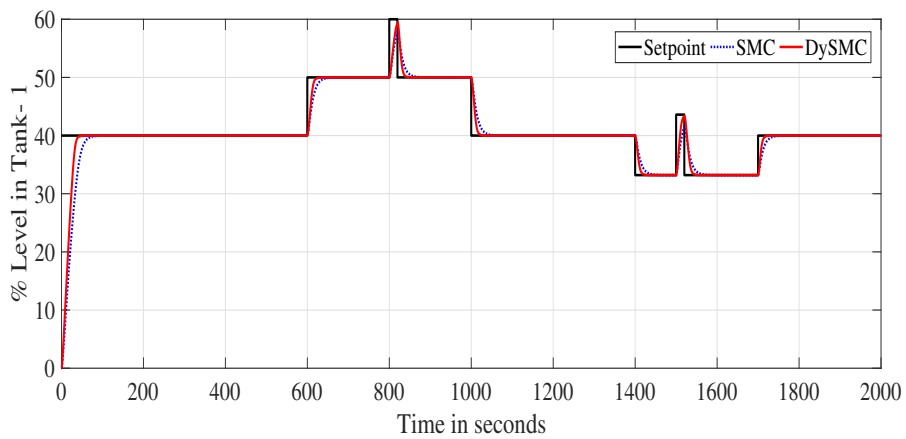


**Fig. 8.** Output response,  $y_1$  for setpoint change, disturbance and under 20% parametric uncertainty

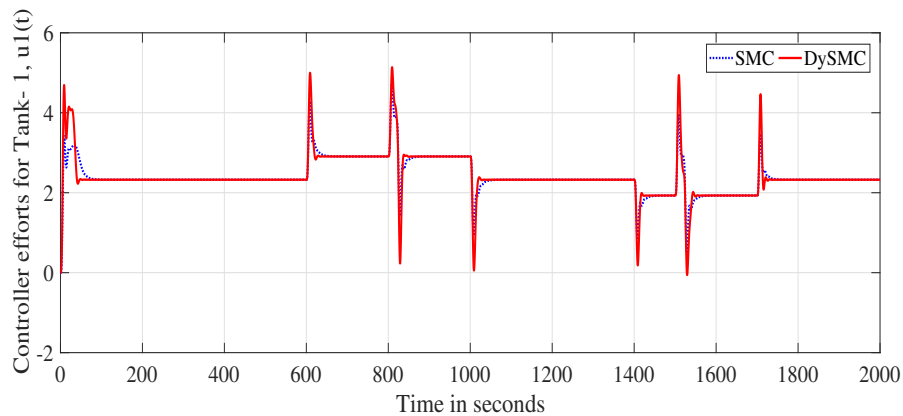


**Fig. 9.** Controller efforts,  $u_1$  for setpoint change, disturbance and under 20% parametric uncertainty

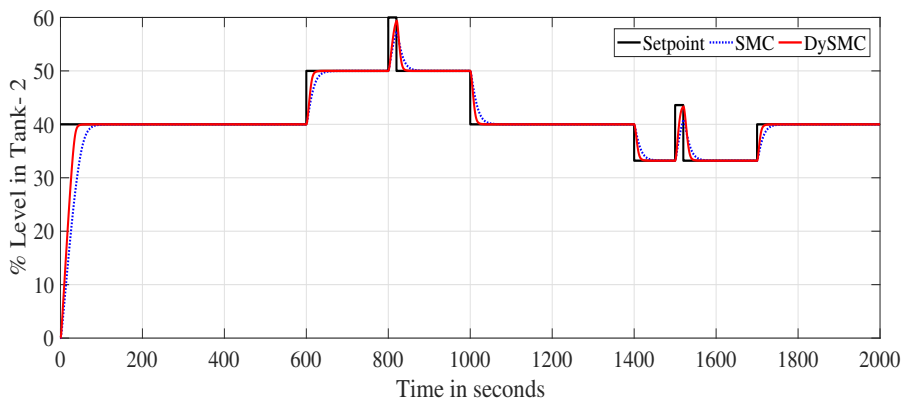


**Fig. 10.** Output response,  $y_2$  for setpoint change, disturbance and under 20% parametric uncertainty

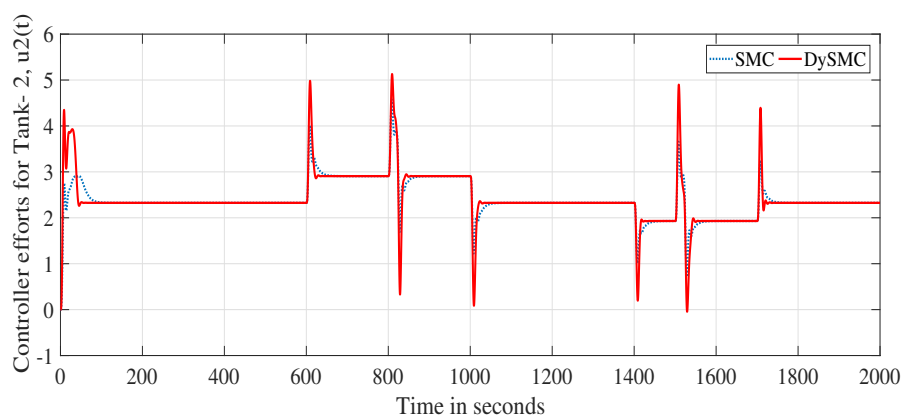


**Fig. 11.** Controller efforts,  $u_2$  for setpoint change, disturbance and under 20% parametric uncertainty

## 5.2. Robustness Test

To assess the performance under parametric deviations, 20% uncertainty is introduced into the system gains, the time constant and delay-time. Fig. 8, Fig. 9, Fig. 10 and Fig. 11 shows the

output and control signals for proposed method and the SMC for both the tanks. Table 3 gives the summary of time-domain specifications with parametric uncertainty and Table 4 gives the summary of performance indices with parametric uncertainty.

**Table 3.** Summary of time domain specifications with parametric uncertainty

Controller	Input ( $u$ ) Output ( $y$ )	Error indices		
		$T_s$	$T_r$	$\%M_p$
DySMC	$u_1 - y_1$	54.16	5.41	0
	$u_2 - y_2$	60.31	5.87	0
SMC	$u_1 - y_1$	90.45	6.58	0
	$u_2 - y_2$	104.07	7.03	0

**Table 4.** Summary of error performance indices with parametric uncertainty

Controller	Input ( $u$ ) Output ( $y$ )	Error indices			
		$IAE$	$ISE$	$ISTAE$	$ISECE$
DySMC	$u_1 - y_1$	27.27	42.57	142.12	95.34
	$u_2 - y_2$	32.69	43.88	194.49	106.22
SMC	$u_1 - y_1$	33.72	46.55	243.28	103.41
	$u_2 - y_2$	37.83	48.29	301.82	108.63

## 6. Real-time Experimentation

Experimental tests are conducted on a nonlinear coupled tank level system to check the applicability and efficiency of the proposed method. Fig. 12 shows laboratory experimental setup. An adjustable valve ( $V_1$ ) is used to have interlinked between the coupled tank. Control valves  $V_2$  and  $V_3$  are provided at the bottom. Level transmitter (LT) have 4 – 20mA supply output which corresponds to 0 – 100% level for each tank [33].



**Fig. 12.** Laboratory setup

For providing flow in each tank, a motor (230v, 50Hz) drives the pump having positive displacement. DAQ card, PCI 6014E, and BNC 2120 connector are used for interfacing the system with personnel computer. Through current to voltage converter, LT is connected to analog input channel BNC 2120. For variable frequency drive (VFD), the controller signal 0 – 5V is converted to 4 – 20mA; through BNC 2120 analog output channel. Using MATLAB/ Simulink, the controller algorithm is implemented. By using the system identification method [3], the transfer function is,

$$G_p(s) = \begin{bmatrix} \frac{0.43}{29s+1}e^{-5s} & \frac{0.145}{40s+1}e^{-10s} \\ \frac{0.172}{35s+1}e^{-10s} & \frac{0.37}{27s+1}e^{-5s} \end{bmatrix} \quad (47)$$

From Eq. (20), decoupler is given by [32],

$$Adj[G_p(s)] = \begin{bmatrix} \frac{0.37}{27s+1}e^{-5s} & \frac{-0.172}{40s+1}e^{-10s} \\ \frac{-0.145}{35s+1}e^{-10s} & \frac{0.43}{29s+1}e^{-5s} \end{bmatrix}$$

$$D(s) = \begin{bmatrix} \frac{e^{5s}}{0.145} & 0 \\ 0 & \frac{e^{5s}}{0.172} \end{bmatrix}$$

$$D_e(s) = \begin{bmatrix} \frac{2.55}{27s+1} & \frac{-1}{40s+1}e^{-5s} \\ \frac{-1}{35s+1}e^{-5s} & \frac{2.5}{29s+1} \end{bmatrix} \quad (48)$$

From Eq. (20), the decoupled systems with the delay approximation gives [34],

$$F_{11}(s) = \frac{1.09649}{(27s+1)(29s+1)(5s+1)} \frac{0.172}{(35s+1)(40s+1)(15s+1)}, \quad (49)$$

$$F_{12}(s) = F_{21}(s) = 0,$$

and

$$F_{22}(s) = \frac{0.925}{(27s+1)(29s+1)(5s+1)} \frac{0.145}{(35s+1)(40s+1)(15s+1)} \quad (50)$$

where,  $F_{11}(s)$  and  $F_{22}(s)$  are of higher orders, therefore they are limited to FOPDT using Eq. (23). From Eq. (24) they can be brought into the form as [34]

$$G_{P11_{FOPDT}} = \frac{0.9245}{113.2s+1}e^{-12.7s} \quad (51)$$

$$G_{P22_{FOPDT}} = \frac{0.78}{113.2s+1}e^{-12.7s} \quad (52)$$

In the design of DySMC, transfer functions are transformed into state space model as

$$\begin{aligned} \ddot{y}_1(t) &= -0.000701y_1(t) - 0.0967\dot{y}_1(t) + u_1(t) \\ \ddot{y}_2(t) &= -0.000654y_2(t) - 0.083\dot{y}_2(t) + u_2(t) \end{aligned} \quad (53)$$

Control signals  $u_1(t)$  and  $u_2(t)$  are given by Eq. (45) and Eq. (46). The control signals are applied to the plant through a decoupler. Consider the FOPDT and decoupled system from Eq. (51) and Eq. (52), the gain margin and phase margin are  $GM > 2.49(8db)$  and  $PM > 59.98^\circ$ . The constants in control law of Eq. (45) and Eq. (46) for the real-time experimentation are taken as:  $c_1=0.8532$ ,  $\lambda_1=5.4310$ ,  $\rho_1=0.046$ ,  $c_2=0.54976$ ,  $\lambda_2=4.417$  and  $\rho_2=0.105$ .

## 6.1. Experimental Results

In this section a reference change, external disturbance, and parametric uncertainty tests are performed on the laboratory coupled tank level process. The aim of control is to maintain a desired level at the setpoint. In this work, the experimental results are performed on Matlab- 2009b software on an Intel core2duo PC, using the ODE4 (Runge-Kutta) solver method with the sampling time of  $T=0.1$  (sec).

### 6.1.1 Multi-level Setpoint Test

Fig. 13 and Fig. 14 shows the nominal response and the controller efforts for Tank-1 without changing the reference input. Similarly, Fig. 15 and Fig. 16 show the responses for Tank-2. Fig. 17 show the output response of Tank-1 when the reference signal is changed from 40% to 50% for 600 seconds to 1000 seconds and 40% to 34% from 1400 seconds to 1700 seconds. Fig. 18 gives the controller efforts of Tank-1 for setpoint change. Similarly Fig. 19 and Fig. 20. output response and controller efforts for Tank-2 for reference change. The summary of the experimental results is tabulated in Table 5.

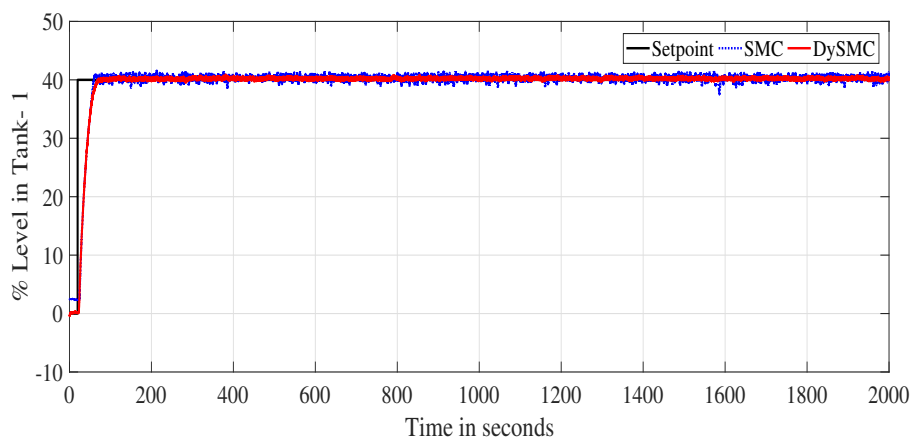


Fig. 13. Output response,  $y_1$  for Tank- 1

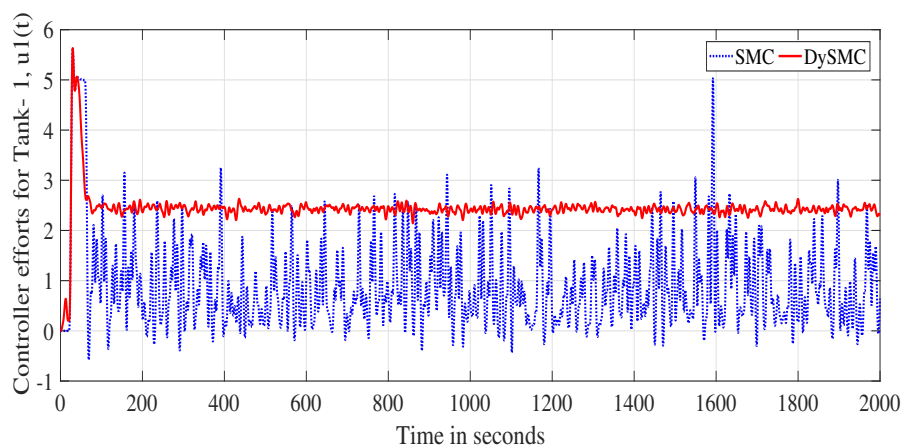
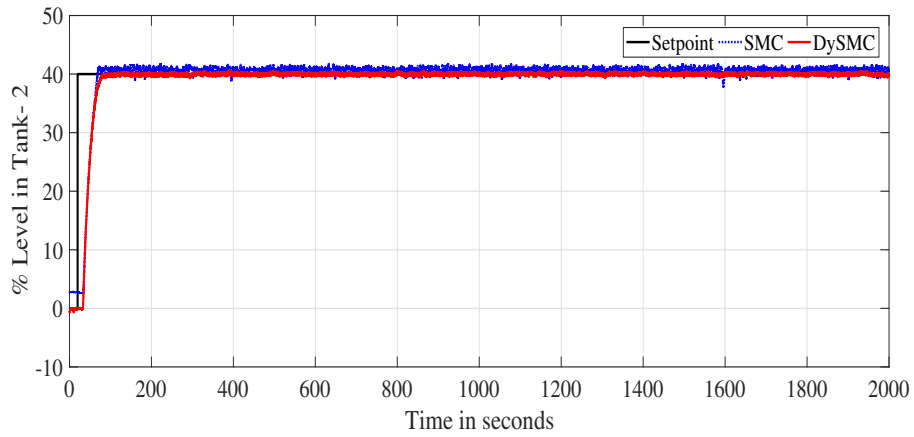
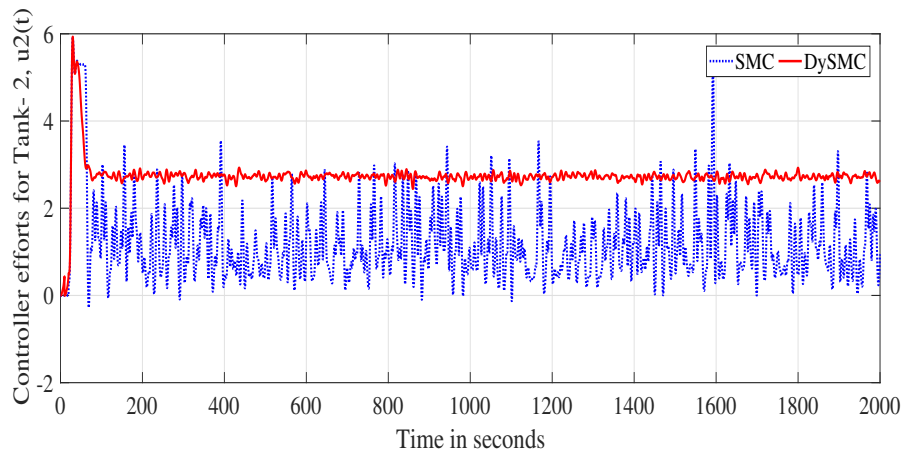


Fig. 14. Controller efforts,  $u_1$  for Tank- 1



**Fig. 15.** Output response,  $y_2$  for Tank- 2



**Fig. 16.** Controller efforts,  $u_2$  for Tank- 2

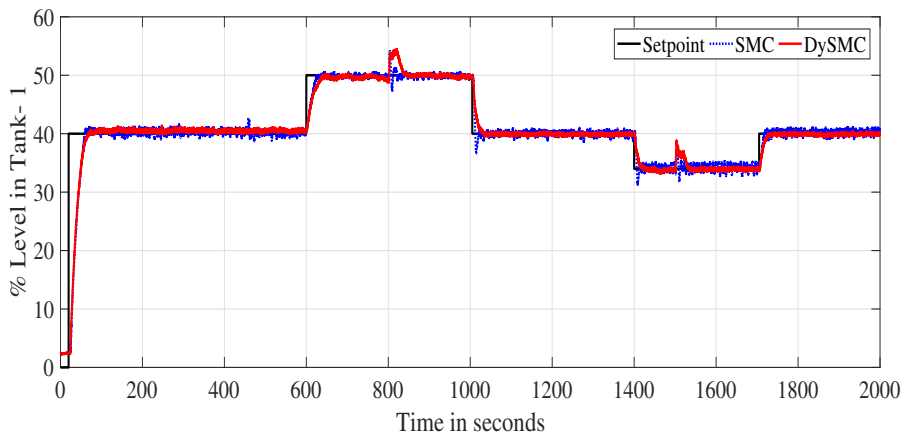


**Fig. 17.** Output response,  $y_1$  for setpoint change and disturbance

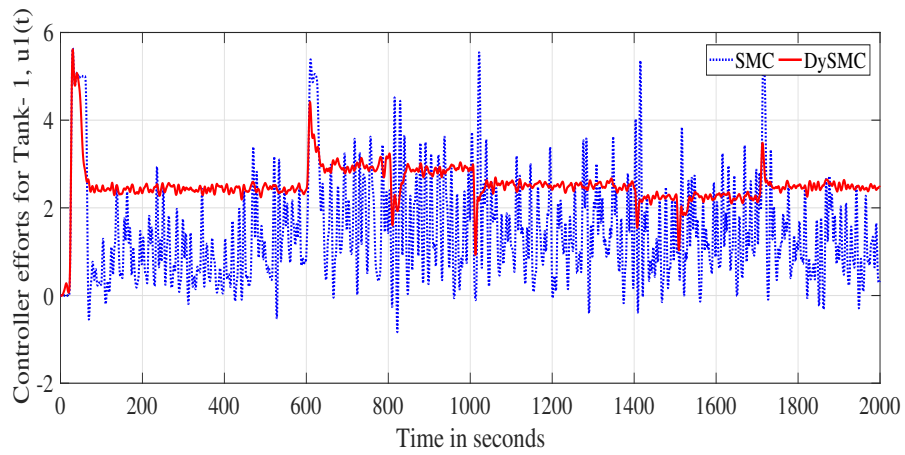


**Fig. 18.** Controller efforts  $u_1$  for setpoint change and disturbance

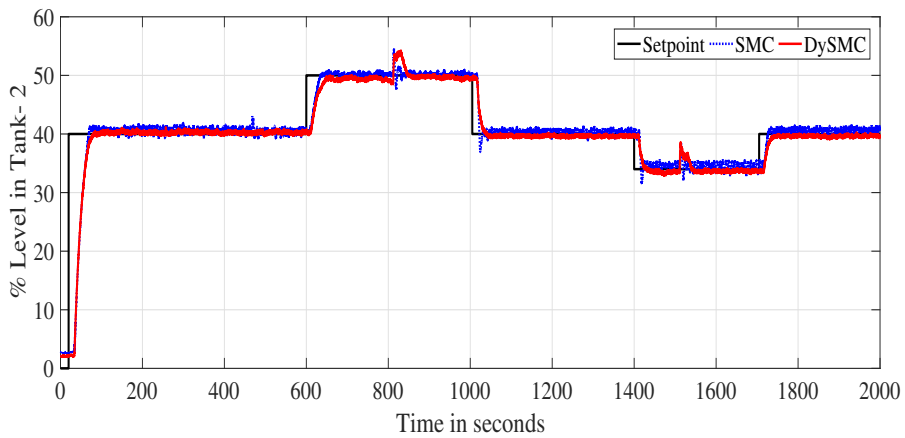


**Fig. 19.** Output response  $y_2$  for setpoint change and disturbance

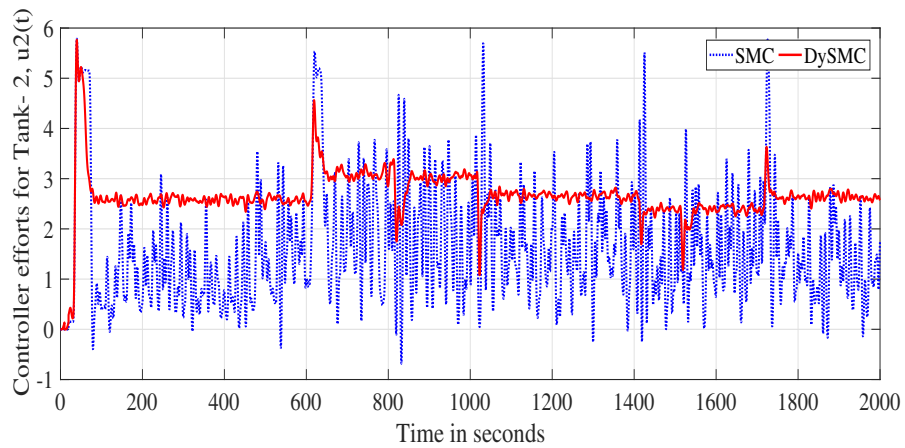


**Fig. 20.** Controller efforts  $u_2$  for setpoint change and disturbance

### 6.1.2 Robustness Test

Fig. 17 and Fig. 18 shows the output response with controller efforts when the external disturbance is added at 800 seconds for 20 seconds and 1500 seconds for 20 seconds for Tank-1. Similarly, Fig. 19 and Fig. 20 shows the output response and the controller efforts for Tank-2 with external disturbance. 20% parametric uncertainty is considered in the plant model for checking the robustness of the proposed controller.

**Table 5.** Summary of the experimental results:  $T_s$ ,  $T_r$ ,  $\%M_p$ ,  $IAE$ ,  $ISE$ ,  $ISTAE$  and  $ISECE$

Controller	Input ( $u$ ) Output ( $y$ )	$T_s$	$T_r$	$\%M_p$	$IAE$	$ISE$	$ISTAE$	$ISECE$
DySMC	$u_1 - y_1$	59.5	24.9	0	85.43	45.82	45.60	$7.1 \cdot 10^7$
	$u_2 - y_2$	65.3	34.9	0	87.56	47.63	48.93	$6.7 \cdot 10^6$
SMC	$u_1 - y_1$	69.71	25.36	0	$3.9 \cdot 10^3$	$7.9 \cdot 10^3$	$2.8 \cdot 10^4$	$5.4 \cdot 10^9$
	$u_2 - y_2$	73.4	36.01	0	$5.2 \cdot 10^3$	$11.6 \cdot 10^3$	$4.2 \cdot 10^4$	$7.3 \cdot 10^9$

## 7. Conclusion

In this paper, DySMC design method for TITO system is explained with numerical simulation and validation is done by performing a real-time experiment on laboratory level system. Employing an ideal decoupler, the interactions are reduced. DySMC controllers are designed independently for each subsystems. In each case the FOPDT model is used. Simulation results show that the proposed controller has achieved a better performance in comparison with traditional SMC against disturbance, setpoint change, and parametric uncertainty. From the experimental study, the proposed controller handles the setpoint change and external disturbances effectively than the conventional one. The proposed approach can reduce chattering effect caused due to the discontinuous component in SMC. The controller response is soft. Since the chattering is eliminated by the proposed controller, the wear and tear of final control elements are also reduced. The procedure for tuning the controller and the parameters taken are tedious and time consuming. Optimization techniques can be used for finding these parameters. Various multi-objective optimization techniques such as NSGA, NSGA-II, NSGA-III, JAYA algorithm etc, can be deployed to choose these tuning parameters, which can improve the performance of the system.

**Author Contribution:** All authors contributed equally to the main contributor to this paper. All authors read and approved the final paper.

**Funding:** This research received no external funding.

**Conflicts of Interest:** The authors declare no conflict of interest.

## References

- [1] C. B. Kadu, A. A. Khandekar, and C. Y. Patil, "Design of sliding mode controller with proportional integral sliding surface for robust regulation and tracking of process control systems," *Journal of Dynamic Systems, Measurement, and Control*, vol. 140, no. 9, 2018, <https://doi.org/10.1115/1.4039468>.
- [2] C. B. Kadu, A. A. Khandekar, and C. Y. Patil, "Sliding mode controller with state observer for tito systems with time delay," *International Journal of Dynamics and Control*, vol. 6, pp. 799–808, 2018, <https://doi.org/10.1007/s40435-017-0342-6>.
- [3] V. Hajare and B. Patre, "Decentralized pid controller for tito systems using characteristic ratio assignment with an experimental application," *ISA Transactions*, vol. 59, pp. 385–397, 2015, <https://doi.org/10.1016/j.isatra.2015.10.008>.

- 
- [4] V. Vijay Kumar, V. Rao, and M. Chidambaram, "Centralized pi controllers for interacting multivariable processes by synthesis method," *ISA Transactions*, vol. 51, no. 3, pp. 400–409, 2012, <https://doi.org/10.1016/j.isatra.2012.02.001>.
- [5] X. Luan, Q. Chen, and F. Liu, "Centralized pi control for high dimensional multivariable systems based on equivalent transfer function," *ISA Transactions*, vol. 53, no. 5, pp. 1554–1561, 2014, <https://doi.org/10.1016/j.isatra.2014.05.016>.
- [6] P. Nordfeldt and T. Hägglund, "Decoupler and pid controller design of tito systems," *Journal of Process Control*, vol. 16, no. 9, pp. 923–936, 2006, <https://doi.org/10.1016/j.jprocont.2006.06.002>.
- [7] S. Tavakoli, I. Griffin, and P. J. Fleming, "Tuning of decentralised pi (pid) controllers for tito processes," *Control Engineering Practice*, vol. 14, no. 9, pp. 1069–1080, 2006, <https://doi.org/10.1016/j.conengprac.2005.06.006>.
- [8] M. Herrera, O. Camacho, H. Leiva, and C. Smith, "An approach of dynamic sliding mode control for chemical processes," *Journal of Process Control*, vol. 85, pp. 112–120, 2020, <https://doi.org/10.1016/j.jprocont.2019.11.008>.
- [9] M. Singla, L.-S. Shieh, G. Song, L. Xie, and Y. Zhang, "A new optimal sliding mode controller design using scalar sign function," *ISA Transactions*, vol. 53, no. 2, pp. 267–279, 2014, <https://doi.org/10.1016/j.isatra.2013.09.007>.
- [10] J. Lee, S.-h. Kim, S. Jung, H. Lee, and Y. Kim, "Sliding mode control design for a multidimensional morphing uav," in *2018 European Control Conference (ECC)*, 2018, pp. 2356–2361, <https://doi.org/10.23919/ECC.2018.8550259>.
- [11] L. Wong, F. Leung, and P. Tam, "A chattering elimination algorithm for sliding mode control," in *Proceedings of the 1996 IEEE IECON. 22nd International Conference on Industrial Electronics, Control, and Instrumentation*, 1996, pp. 264–268, <https://doi.org/10.1109/IECON.1996.570963>.
- [12] J.-L. Chang, "On chattering-free dynamic sliding mode controller design," *Journal of Control Science and Engineering*, vol. 2012, 2012, <https://doi.org/10.1155/2012/564906>.
- [13] J. Hu, H. Zhang, H. Liu, and X. Yu, "A survey on sliding mode control for networked control systems," *International Journal of Systems Science*, vol. 52, no. 6, pp. 1129–1147, 2021, <https://doi.org/10.1080/00207721.2021.1885082>.
- [14] H. Sira-Ramirez, "On the dynamical sliding mode control of nonlinear systems," *International Journal of Control*, vol. 57, no. 5, pp. 1039–1061, 1993, <https://doi.org/10.1080/00207179308934429>.
- [15] G. Bartolini and P. Pydynowski, "An improved, chattering free, vsc scheme for uncertain dynamical systems," *IEEE Transactions on Automatic Control*, vol. 41, no. 8, pp. 1220–1226, 1996, <https://doi.org/10.1109/9.533691>.
- [16] G. Bartolini, A. Ferrara, E. Usai, and V. Utkin, "On multi-input chattering-free second-order sliding mode control," *IEEE Transactions on Automatic Control*, vol. 45, no. 9, pp. 1711–1717, 2000, <https://doi.org/10.1109/9.880629>.
- [17] S. Sankeswari and R. Chile, "Sliding mode approach for performance improvement of slow and fast dynamic uncertain systems," *Int. J. Autonomic Comput.*, vol. 3, no. 2, p. 87–113, 2018, <https://doi.org/10.1504/IJAC.2018.097615>.
- [18] O. Simeone, Q.-G. Wang, C. Lin, and T. Lee, *Relay Feedback: Analysis, Identification and Control*. Springer, 2003, <https://doi.org/10.1007/978-1-4471-0041-6>.
- [19] D. Dougherty and D. Cooper, "A practical multiple model adaptive strategy for single-loop mpc," *Control Engineering Practice*, vol. 11, no. 2, pp. 141–159, 2003, [https://doi.org/10.1016/S0967-0661\(02\)00106-5](https://doi.org/10.1016/S0967-0661(02)00106-5).
- [20] V. Utkin, "Variable structure systems with sliding modes," *IEEE Transactions on Automatic Control*, vol. 22, no. 2, pp. 212–222, 1977, <https://doi.org/10.1109/TAC.1977.1101446>.
- [21] J. Liu and X. Wang, *Advanced sliding mode control for mechanical systems*. Springer, 2011, <https://doi.org/10.1007/978-3-642-20907-9>.
-

- 
- [22] J. Liu, Y. Li, and Z. Yang, "A dynamic sliding mode control method for multi-agent formation," *Journal of Physics: Conference Series*, vol. 1754, no. 1, p. 012101, 2021, <https://doi.org/10.1088/1742-6596/1754/1/012101>.
- [23] O. Camacho and R. Rojas, "A general sliding mode controller for nonlinear chemical processes," *Journal of Dynamic Systems, Measurement, and Control*, vol. 122, no. 4, pp. 650–655, 02 2000, <https://doi.org/10.1115/1.1318351>.
- [24] Y. Fang, W. Fu, C. An, Z. Yuan, and J. Fei, "Modelling, simulation and dynamic sliding mode control of a mems gyroscope," *Micromachines*, vol. 12, p. 190, 2021, <https://doi.org/10.3390/mi12020190>.
- [25] Z. Xi, "Dynamic sliding mode controller design for networked control systems with random packet loss and event driven quantisation," *IET Control Theory & Applications*, vol. 12, no. 17, pp. 2433–2440, 2018, <https://doi.org/10.1049/iet-cta.2018.5572>.
- [26] P. Suryawanshi, P. Shendge, and S. Phadke, "Robust sliding mode control for a class of nonlinear systems using inertial delay control," *Nonlinear Dynamics*, vol. 78, pp. 1921–1932, 2014, <https://doi.org/10.1007/s11071-014-1569-9>.
- [27] M. Das and C. Mahanta, "Optimal second order sliding mode control for linear uncertain systems," *ISA Transactions*, vol. 53, no. 6, pp. 1807–1815, 2014, <https://doi.org/10.1016/j.isatra.2014.08.010>.
- [28] M. G. Ghogare, S. L. Patil, and C. Y. Patil, "Experimental validation of optimized fast terminal sliding mode control for level system," *ISA Transactions*, 2021, <https://doi.org/10.1016/j.isatra.2021.08.007>.
- [29] J.-J. E. Slotine and W. Li, *Applied Nonlinear Control*. Prentice-Hall, 1991, <https://books.google.co.id/books?id=cwpRAAAAMAAJ>.
- [30] R. Kavikumar, B. Kaviarasan, Y.-G. Lee, O.-M. Kwon, R. Sakthivel, and S.-G. Choi, "Robust dynamic sliding mode control design for interval type-2 fuzzy systems," *Discrete and Continuous Dynamical Systems-S*, 2022, <https://doi.org/10.3934/dcdss.2022014>.
- [31] I.-L. Chien, H.-P. Huang, and J.-C. Yang, "A simple multiloop tuning method for pid controllers with no proportional kick," *Industrial & Engineering Chemistry Research*, vol. 38, pp. 1456–1468, 1999, <https://doi.org/10.1021/ie980595v>.
- [32] A. Khandekar and B. Patre, "Decentralized discrete sliding mode controller for tito processes with time delay with experimental application," *International Journal of Dynamics and Control*, vol. 5, 2017, <https://doi.org/10.1007/s40435-015-0202-1>.
- [33] M. Ghogare, S. Patil, C. Patil, A. Laware, and L. Chaudhari, "Design and experimental validation of non-singular terminal sliding mode control for level control system," in *2021 IEEE 18th India Council International Conference (INDICON)*, 2021, pp. 1–6, <https://doi.org/10.1109/INDICON52576.2021.9691606>.
- [34] V. Hajare, B. M. Patre, A. Khandekar, and G. Malwatkar, "Decentralized pid controller design for tito processes with experimental validation," *International Journal of Dynamics and Control*, vol. 4, pp. 583–595, 2017, <https://doi.org/10.1007/s40435-016-0252-z>.